International Association of Geodesy Symposia

Volume 131

F. Sansò
A. J. Gil
(Eds.)

Geodetic Deformation Monitoring: From Geophysical to Engineering Roles

IAG Symposium
Jaén, Spain
March 17–19, 2005

Springer

Studies on Crustal Structure and Gravity in the Eastern Alps

E. Brückl, U. Mitterbauer, M. Behm
Institute of Geodesy and Geophysics
Vienna University of Technology, Gusshausstrasse 27-29, 1040 Vienna, Austria

CELEBRATION 2000 and ALP 2002 Working Groups
http://paces.geo.utep.edu/celebration_web/celebration.shtml; http://www.alp2002.info

Abstract. This study concentrates on the Eastern Alps and their transition into the surrounding Bohemian Massif, the Pannonian Basin, the Carpathians and the Dinarides. The geodynamic setting is characterized by the ~N-S directed head-on collision between the European and Adriatic-Apulian plates in the central part of the Eastern Alps, leading to the E-directed lateral extrusion of the Eastern Alps into the Pannonian Basin, and the transition of the Eastern Alps to the Dinarides. New seismic data about the lithosphere in this area has been derived from the wide-angle reflection and refraction experiments CELEBRATION 2000 and ALP 2002. A 3D model of the P-wave crustal velocity has been generated by tomographic methods. Further, a map of the Moho discontinuity has been constructed. Both stacking techniques and travel time inversion have been applied. Interactive modeling by 2D ray tracing along selected lines has been used to supplement the 3D evaluation. The tomographic model of the crust supplies continuous information about the P-wave velocity only in the upper crust. Bouguer gravity data has been implemented to better constrain the velocity of the lower crust by the use of a velocity-density relation. For the uppermost 10 km, the density has been derived from the seismic model. For the lower crust, a linear velocity-depth function has been deduced removing the gravity effect of the Moho topography from the Bouguer gravity. The residual gravity shows a significant regional pattern that can be related to geologic provinces (e.g. Bohemian Massif, Molasse, Pannonian Basin, and Vienna Basin) and the geodynamic situation (existence of a tectonic block forming a triple junction with the European and Adriatic-Apulian plates). An integrated model has been constructed, which fits well seismic and gravimetric data and is very close to Airy-isostatic equilibrium.

Keywords. Eastern Alps, crust, Moho, reflection and refraction seismology, gravity, isostasy.

1 Introduction

The target of this study is the lithosphere of the Eastern Alps and their transition into the Bohemian Massif, the Pannonian Basin, the Carpathians and the Dinarides (Figure 1). The geodynamic setting is characterized by the approximately N-S directed head-on collision between the European and Adriatic-Apulian plates in the central part of the Eastern Alps. This collision started in the Oligocene. Continued convergence through the Tertiary led to the present orogenic pattern. The continent-continent collision is not the only imprinting tectonic process. In the late Oligocene and Miocene, lateral escape took place from the compressed Central Alps to the unconstrained margin of the Pannonian Basin. The significant eastward thinning of the crust corresponds to the extrusion and tensional processes (Ratschbacher et al., 1991). The present day seismicity in the area of our investigation follows a pattern compatible with the escape tectonic model (Aric et al., 1987).

Seismic exploration of the lithosphere of the Eastern Alps has a long tradition. Refraction and wide-angle reflection experiments started around the Eschenlohe quarry 40 years ago. Seismic lines spread out from this shot point over the Alps to the shot points Lago Lagorai and Trieste (Giese et al., 1976). The projects ALP 75, ALP 77, and ALP 78 supplied further refraction and wide-angle reflection lines (Yan and Mechie 1989; Scarascia and Cassinis 1997). Deep reflection seismic profiling started in former Czechoslovakia in 1980. The profiles 3T and 8HR (Tomek 1993a, 1993b) focused on the transition from the Bohemian Massif to the Carpathians and the Pannonian Basin. In Hungary, the Pannonian Basin was explored by deep reflection seismic profiling during the occasion of the Pannonian Geotraverse (Posgay et al., 1996). In Austria, deep reflection seismic profiling was carried out in the area of the Rechnitz Penninic window in NE Styria (Weber et al. 1996; Graßl et al. 2004). An important deep reflection line

bounding the investigation area of this study to the W is TRANSALP (Transalp Working Group 2002), which crosses the Eastern Alps from Munich to Verona. The most recent results on the seismic structure derive from the 3D refraction experiments CELEBRATION 2000 (Guterch et al. 2003) and ALP 2002 (Brückl et al. 2003a). Preliminary 2D- and 3D-models of the crust and Moho are available from these two experiments.

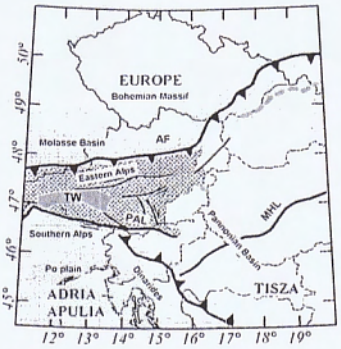

Fig. 1 Tectonic setting of the investigation area
PAL: Periadriatic Lineament
AF: Alpine Front
MHL: Mid-Hungarian Line
TW: Tauern Window

Gravimetric investigations have also supplied valuable information on the structure of the Eastern Alpine crust. Before 1973 gravity measurements in the Eastern Alps were performed mainly along the benchmarks of leveling lines. A Bouguer gravity map of Austria was derived from approximately 2000 stations by Senftl (1965). In 1973 a densification of the gravity net and modeling started in Austria with the Gravimetric Alpine Traverse (Meurers et al. 1987). Another study by Meurers (1993) covered the plutonic and metamorphic part of the Bohemian Massif in Austria. Lillie et al. (1994) focused on regional studies on gravity and isostasy, extending from the Eastern Alps to the Carpahtians and Pannonian Basin. One profile, crossing the Alps from N to S at 13°E longitude and another, W-E oriented at 47° latitude cover the investigation area of this study. The Eschenlohe-Trieste (NW-SE) and Eschenlohe-Vicenza (N-S) seismic profiles were used as a basis for a density model and as constraints for a gravity inversion by Braitenberg et al. (1997) and Dal Moro et al. (1998). The 3D density model along the TRANSALP profile was developed by Ebbing et al. (2001), Ebbing (2002), and Ebbing (2004). The model was then used for calculating internal crustal loads and evaluate the elastic thickness variations and the isostatic equilibrium in the frame of the flexural isostatic model in Braitenberg et al. (2002).

In this paper we present preliminary seismic models of the crust and the Moho derived from CELEBRATION 2000 and ALP 2002 data. Information on the P-wave velocity of the lower crust is incomplete or not very reliable. Gravity data will be used as a constraint on the velocity of the lower crust. The implementation of the gravimetric data into the seismic model will be described and a correlation of the main structural features with the regional geology and geodynamic situation will be attempted.

2 Preliminary Seismic Model of the Eastern Alps Derived from CELEBRATION 2000 and ALP 2002 Data

In this study we consider a merged data set from the 3rd deployment of CELEBRATION 2000 (55 shots, 844 receivers, total profile length 2 800 km) and ALP 2002 (39 shots, 947 receivers, total profile length 4 300 km) (Figure 2). This data set comprises more than 78,000 traces.

2D-interpretations by interactive ray tracing modeling (Červený, V. and I. Psencik 1984) have been published for the line CEL09 (Hrubcová et al, 2005). Preliminary interpretations of Alp01 and Alp02 have been presented as a poster (Bleibinhaus et al., 2004).

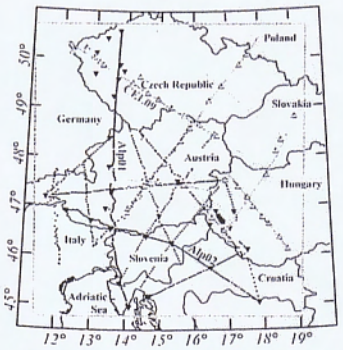

Fig. 2 Field layout of CELEBRATION 2000, 3rd deployment (grey) and ALP 2002 (black). Shots are shown as triangles, receivers as dots; the lines CEL09 and Alp01 and Alp02 are labeled.

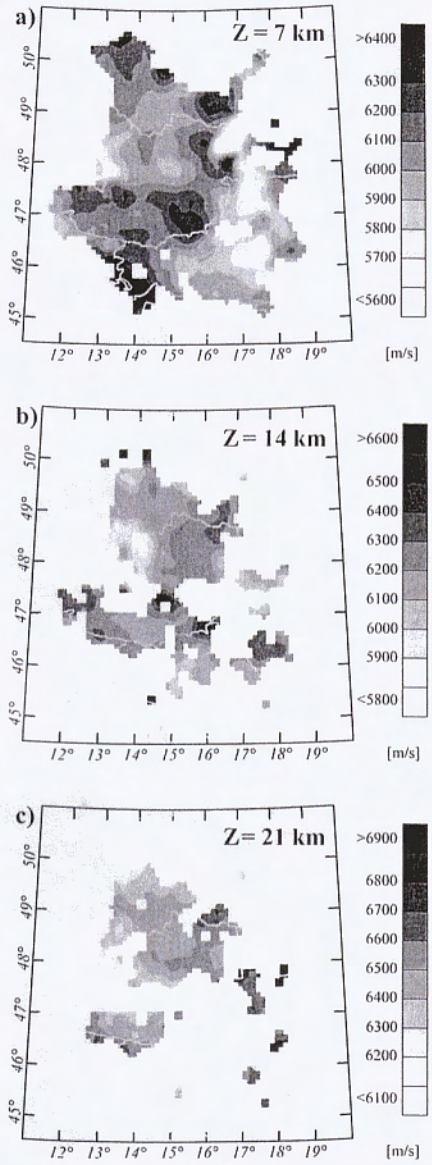

Fig.3 Depth slices through the 3D P-wave velocity model of the crust in (a) 7 km, (b) 14 km, and (c) 21 km depth.

A 3D P-wave velocity model of the crust has been derived from Pg-diving wave tomography as well as a map of the Moho discontinuity from Pn delay time analysis and PmP wide-angle reflections. Both stacking techniques to improve signal to noise ratio and travel time inversions were applied. The methods used were presented at the AGU fall meeting (Brückl et al. 2003b) and are described in detail in Behm (2006). Horizontal slices through the P-wave velocity model of the crust at 7, 14 and 21 km depth are shown in Figures 3a-c.

Significant velocity structures can be recognized, which correlate well with the regional tectonic setting. Low velocities down to about 7 km depth are found in the Pannonian Basin. Other velocity lows corresponding to the Molasse Basin, the Vienna Basin and the granite part of the Bohemian Massif reach below 10 km. The most prominent velocity high is in and north of Istria; others are the metamorphic part of the Bohemian Massif and an E-W stretching zone N to the central range of the Eastern Alps. These velocity highs reach below 10 km. The transition from the Diarides in N to the Tisza unit in S (Mid Hungarian Line) can be identified by an increase of velocities at depths around 10 km.

The analysis of the Pn delay times and the wide-angle PmP reflections have been referenced to the depth datum Z=10 km. The average and standard deviation of the Pn velocity is 7990 +/- 90 ms^{-1}. Figure 4 shows a map of the Pn-velocity. Low velocities can be found in an E-W oriented belt at the northern front of the Eastern Alps. Another area of low Pn velocities is the Croatian part of the Pannonian Basin. The highest Pn velocities are below Istria (Adriatic-Apulian plate) and the central part of the Bohemian Massif.

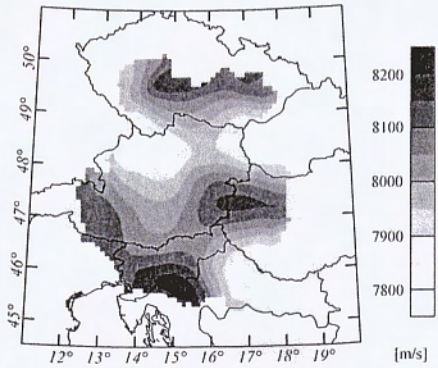

Fig. 4 Upper mantle velocity derived from a delay time analysis of the Pn-phase.

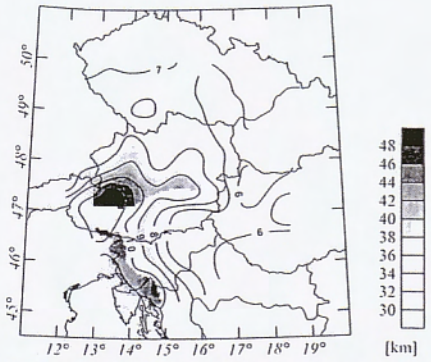

Fig. 5 Moho depth map derived from Pn delay time analysis and PmP wide-angle reflection processing (grey); iso-lines refer to vertical (migrated) 2-way Moho reflection travel time T0, reference datum Z = 10 km.

Figure 5 shows a map of the Moho discontinuity. The Moho depth is visualized by a grey code. Additionally, iso-lines of the vertical (or migrated) 2-way Moho reflection travel time, referenced to the datum Z = 10 km are superimposed. This transformation to the time domain makes the Moho map insensitive against errors in the velocities of the lower crust and will serve as "hard" information on the Moho in our later considerations.

A preliminary interpretation of the Moho structure is an S-dipping European Moho, underthrusting the Adriatic Moho from the western boundary of the investigation area to about 14°E. Further to the E we introduced a tectonic block or microplate, which is underthrusted by the European plate from the N and the Adriatic-Apulian plate from the SSW. This tectonic block shall be called "Pannonia" in the following. Scarascia and Cassinis (1997) separated this fragment as "Thin Adriatic Moho" from the surrounding Moho parts. A maximum Moho depth of about 50 km is found at the triple junction between the European and Adriatic-Apulian plate and "Pannonia", a minimum Moho depth of 27 km is found in the southern Pannonian Basin.

Support for the suggested 3D Moho model comes also from the 2D-interpretations by interactive ray tracing along ALP75 (Yan and Mechie, 1989), CEL09 (Hrubcová et al. 2005) and the preliminary results from Alp01 and Alp02 (Bleibinhaus et al. 2004). The difference in Moho depth between the independently derived 2D and 3D evaluations is about 1.0 +/- 2.0 km. The high crustal velocities of the Adriatic-Apulian plate were also verified by the 2D interpretations. Teleseismic tomography in this area (Lippitsch 2002, Lippitsch et al. 2003; Schmid et al. 2004) indicates a change in the direction of the subduction. According to these results and interpretations W of TRANSALP the European plate is subducted below the Adriatic-Apulian plate. Roughly at TRANSALP the direction of subduction changes and E of TRANSALP the Adriatic-Apulian plate is subducted below Europe. At present we cannot conclude whether a tectonic model in agreement with Moho structure shown in Figure 5 and the teleseismic model can be constructed.

3 Constraining the P-Wave Velocity of the Lower Crust by Gravity

The tomographic model of the crust supplies nearly continuous information about the P-wave velocity only in the uppermost 10 km of the crust. In most areas the diving wave tomography does not penetrate down to the Moho (Figure 6). A preliminary model of the average P-wave velocity of the crust between Z = 10 km and the Moho (Figure 7) has been constructed by estimating the P-wave velocity between the maximum penetration depth and the Moho from RMS-velocities (V_{RMS}) of PmP phases and constraints from global data (Christensen and Mooney, 1995). The map of the Moho in time and depth domain (Figure 5) has been constructed by the use of this preliminary velocity model.

An additional constraint on the P-wave velocity of the lower crust (below the penetration depth of the diving wave tomography) can be derived from gravity assuming a relation between P-wave velocity and density. The Christensen and Mooney (1995) velocity-density relationship is based on a world wide collection of refraction and wide-angle reflection data. Using this relation we do not consider the influence of the geothermal gradient or the mineralogy. Sobolev and Babeyko (1994) derived a relation between P-wave velocity and density that considers the thermal gradient and the mineral transformations within the crust with changing PT conditions. Ebbing (2002) used this relation together with the regional heat-flow data supplied by Cermak et al. (1992) for the 3D modeling of the gravity in the area TRANSALP (Eastern Alps between 10° - 14° E). However, only few observations on the geothermal gradient are available within the Eastern Alps (Sachsenhofer 2001). The additional use of S-wave velocity or Poisson's ratio could resolve to some degree the

influence of mineral composition (Christensen 1996). The evaluation of S-wave velocities and Poisson's ratios will be possible from the CELEBRATION 2000 and ALP 2002 data in the future. The implementation of the gravity constraints presented in this paper has the character of a pilot study. Therefore we decided to choose the Christensen and Mooney (1995) velocity-density relationship because only P-wave velocity data are needed to estimate crustal densities. These simplifications must be kept in our mind in our later interpretations.

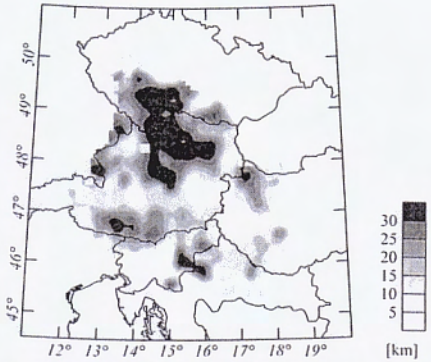

Fig. 6 Penetration depth of Pg-diving wave tomography.

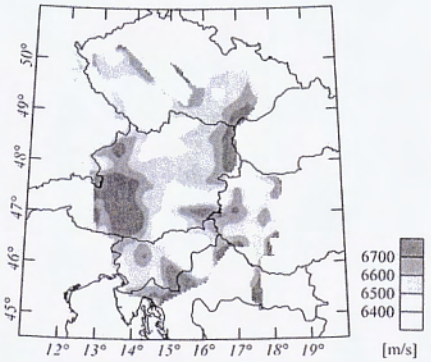

Fig. 7 Preliminary model of the average P-wave velocity of the crust between Z = 10 km and the Moho.

The gravity data used in this study (Figure 8) is the regional Bouguer gravity map of the West East European Gravity Project (http://www.getech.com). Within Austria this data has been replaced by the "New Austrian Bouguer Map" (Kraiger and Kühtreiber 1992). We call the Bouguer gravity derived from this data dgB0. The density for reduction of masses above the Ellipsoid is d = 2670 kg/m^3.

The following steps will be carried out in order to constrain the P-wave velocity of the lower crust by gravity:

· Stripping of the uppermost 10 km of the crust yielding the Bouguer gravity residuum dgB1.

· Subtracting the gravity effect of the lower crust yielding the residuum dgB2; an average linear velocity-depth function of the lower crust and corresponding densities are determined by the condition such that the correlation coefficient between dgB2 and T0 (Moho depth in time domain) is zero.

· Modeling the Bouguer gravity residuum (dgB2) by masses in the lower crust and derivation of corresponding variations of the P-wave velocity.

· Combination of the interval velocities of the lower crust (between Z = 10 km and the Moho) derived from seismic and gravimetric data.

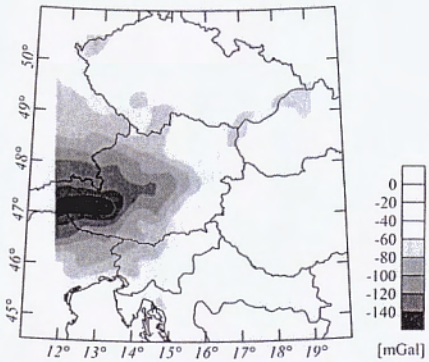

Fig. 8 Bouguer gravity map of the investigation area compiled from data of the West East European Gravity Project and the "New Austrian Bouguer Map" (for references see text).

Gravity modeling will be done by a superposition of the gravity effects of prismatic bodies after Nagy (1966). Densities relative to a reference model will be used in order to avoid edge effects. The steps for the implementation of the constraints from gravity in order to resolve the P-wave velocity of the lower crust will be described in detail in the following chapters.

4 Stripping the Uppermost 10 km of the Crust

Between the surface and the level Z = 10 km the 3D P-wave velocity model covers almost the whole area. Therefore, the densities are well constrained by the P-wave velocities. The calculation of the gravity effect is straight forward (Figure 9) without the need of assumptions. The reference density for the uppermost 10 km of the crust is 2670 kg/m^3. Subtraction of this gravity effect from the Bouguer gravity dgB0 yields a residual gravity dgB1 (Figure 10) that still shows the effect of the varying depth of the Moho, but also additional masses below sedimentary basins, compensating the mass deficit of the sediments. Such a gravity signal can be detected below the Vienna and Pannonian Basins.

The implementation of the detailed surface density map of Austria (Steinhauser et al. 1984) into the stripping of the uppermost 10 km of the crust could improve the result. However, proper weighting of densities derived from near surface samples and from P-wave velocity is a task beyond the scope of this study.

5 Average Linear Velocity Function of the Lower Crust

Moho depths have been calculated by the assumption of the following parameters of a linear velocity-depth function, valid below Z = 10 km.
P-wave velocities at Z = 10 km (V_{10km}): 5900, 6000, 6100, 6200, 6300 ms^{-1}; vertical velocity gradients (k): 0.10, 0.15, 0.20, 0.25, 0.30 s^{-1}.

For these 25 velocity-models of the lower crust we calculated also the densities and the gravity effect of the masses between Z = 10 km and the Moho assuming two values for the upper mantle density, d_M=3250 kg m^{-3} and d_M=3300 kg m^{-3}. Subtraction of these gravity effects from dgB1 yields the residual Bouguer gravity dgB2. A lower crust density of 2900 kg m^{-3} and a Moho depth of 33 km were used as reference. The reference density of the upper mantle was always the density d_M of the model.

We assume that the best choice for an average velocity-depth function of the lower crust yields minimum correlations between dgB2 and T0, the time information on the Moho depth (migrated 2-way reflection travel time). The signature of the varying crustal thickness will be removed by this choice. The assumption has been made, that there are no deeper (upper mantle) density structures that produce a correlation between dgB2 and T0.

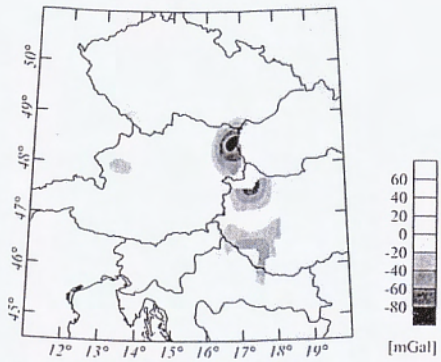

Fig. 9 Gravity effect of the upper crust (Z <= 10 km).

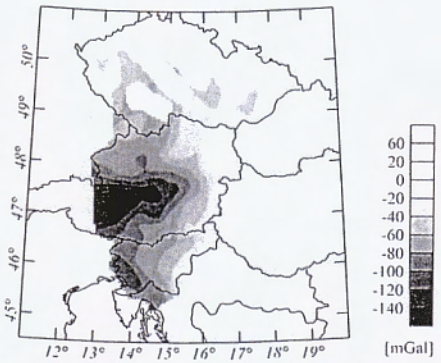

Fig. 10 Residual gravity dgB1 after stripping the upper crust (Z <= 10 km).

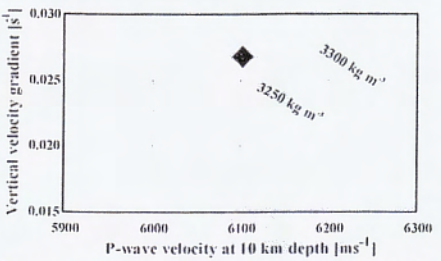

Fig. 11 Parameter combinations (grey lines) of linear velocity-depth functions for the lower crust (between 10 km depth and the Moho) that yield zero correlation between T0 (two way vertical travel time to Moho, datum Z = 10 km) and dgB2 (Bouguer gravity residuum after correction for the crust) for two mantle densities 3250 and 3300 kg m^3; the diamond represents the world wide average for orogens (Christensen and Mooney 1995).

The idea of our method is similar to Nettleton's method to determine the density of topographic masses by minimizing the correlation of the Bouguer anomaly with the terrain elevation. Figure 11 shows the pairs of V_{10km} and k that result in zero correlation between dgB2 and T0. We see there is an ambiguity in a sense that either lower V_{10km} and higher k, or higher V_{10km} and lower k result in zero correlation. In order to get additional constraints on V_{10km} and k we approximated the world wide average velocities for orogens (Christensen and Mooney 1995) by a linear velocity-depth function and plotted the corresponding values for V_{10km} = 6102 ms^{-1} and k = 0.0268 s^{-1} in the same diagram. With this velocity function for the crust below 10 km depth and an upper mantle density d_M = 3270 kgm^3 we also yield a zero correlation of dgB2 with T0. Therefore we take this parameter triple as our optimum solution. The average velocity of our 3D seismic model at Z = 10 km is 6090 ms^{-1}, which is in good agreement with this choice. The residual gravity dgB2 for these optimum parameters is shown in Figure 12.

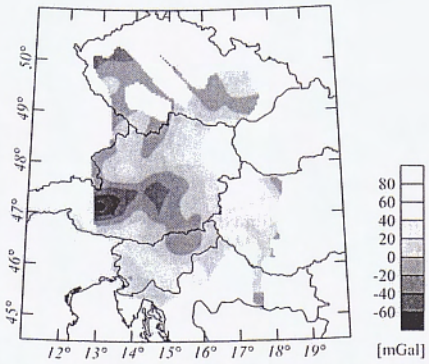

Fig. 12 Residual gravity (dgB2) after subtracting the effect of the lower crust with an average linear velocity function.

6 Modeling of the Bouguer Gravity Residuum

The Bouguer gravity residuum (dgB2) can be related to tectonic structures. An anomaly low correlates with the South Bohemian Pluton that has significantly lower densities than the metamorphic part of the Bohemian Massif (Meurers 1993). Corresponding variations of the P-wave velocity can be traced below 10 km depth in our 3D seismic model. Gravimetric modeling (Meurers 1993) also confirms that the sources of this anomaly are distributed over a depth range of at least 10 km. Another well-known anomaly is the gneiss kernel of the Tauern Window. Quantitative modeling of the low density body of the Tauern Window (Ebbing 2000) limit these low densities to the uppermost 10 km of the crust. The 3D seismic model does not show a corresponding low in the velocities of the upper crust.

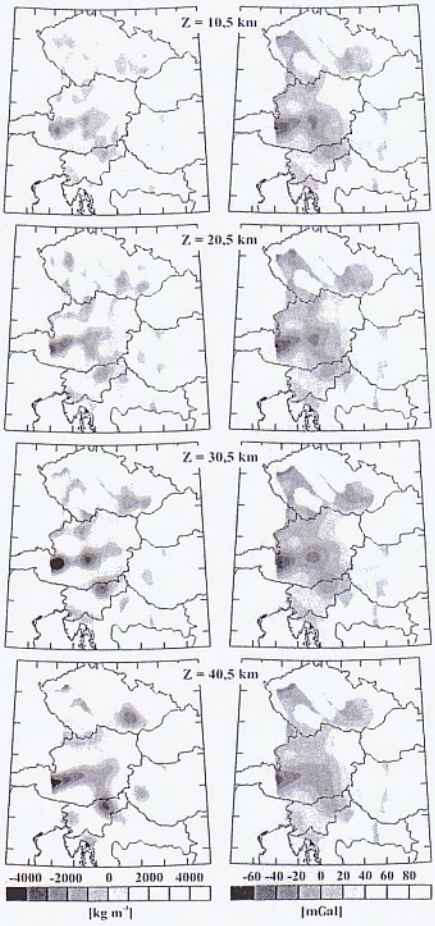

Fig. 13 Modeling of residual gravity by sources in 1 km thick layers at 4 depth levels between 10.5 and 40.5 km; left column shows the model densities of the 1 km thick layers, right column the calculated gravity effect of these layers.

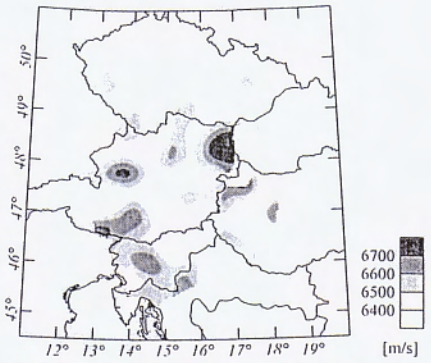

Fig. 14 Average P-wave velocity V_{grav} of the crust between Z = 10 km and the Moho derived from gravimetric data.

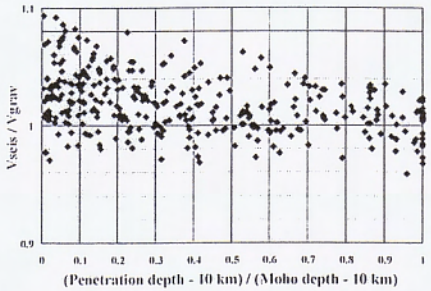

Fig. 15 Ratio R of V_{seis} (seismically determined average velocity of the lower crust) to V_{grav} (gravimetrically determined average velocity of the lower crust) versus the ratio of penetration depth to crustal thickness.

Evidence for an Adriatic-Apulian plate dipping below the assumed tectonic block "Pannonia" and the Dinarides is indicated by positive anomalies. Strong positive anomalies are also found in the transition from the Northern Pannonian domain and the Vienna Basin to the European platform, where also high velocities in the lower crust are obtained from the seismic model.

In order to get an estimate of the geologically reasonable depth range of the sources, we modeled the residual Bouguer gravity (dgB2) by masses concentrated in one layer of 1 km thickness at the depth levels of Z = 10.5, 20.5, 30.5, and 40,5 km (Figure 13).

As to be expected, the shallowest distribution of sources models the residual gravity best, but also down to Z = 30.5 km the calculated distribution of masses are geologically reasonable and fit the data well. At Z = 40.5 km the distribution of masses becomes less geologically reasonable. Thus we conclude that it is geologically reasonable to distribute the sources of the residual Bouguer gravity (dgB2) evenly over the depth range of the lower crust. Conversion of the resulting density changes to velocity changes and adding these improvements to the average linear P-wave velocity function of the lower crust results in V_{grav}, the gravimetrically determined interval velocity between the datum Z = 10 km and the Moho (Figure 14). The values of V_{grav} at the location of the Tauern Window will be excluded from our further analysis, because the source of dgB2 is the gneiss kernel in the uppermost 10 km of the crust and must not be projected to the lower crust.

7 Combination of Seismic and Gravimetric Velocity Information on the Lower Crust

Figure 15 shows the ratio V_{seis}/V_{grav} versus the ratio R of penetration depth below Z = 10 km to thickness of the lower crust (Between Z = 10 km and Moho). It is evident, the greater the penetration depth of the diving wave tomography, the less differs the ratio V_{seis}/V_{grav} from unity. The ratio V_{seis}/V_{grav} is 1.003 +/- 0.018 for R>0.85. We therefore construct a velocity solution from a weighted mean of V_{seis} and V_{grav} seismic solution (Figure 16): $V_{seis+grav} = R \cdot V_{seis} + (1-R) \cdot V_{grav}$. Because of the weighting scheme, the seismic information about the lower crust is not changed where information from diving wave tomography is available down to the Moho.

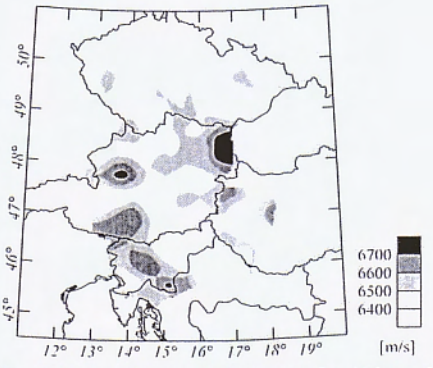

Fig. 16 Average P-wave velocity between Z = 10 km and Moho derived from seismic and gravimetric data.

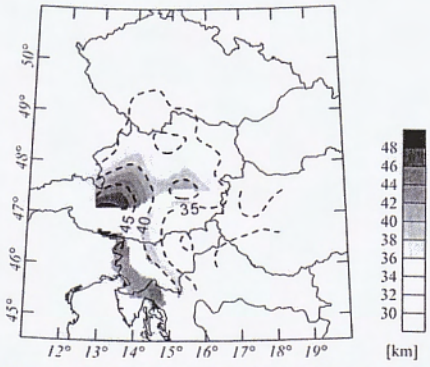

Fig. 17 Moho depth map calculated by the use of the combined seismic-gravimetric velocity model of lower crust.

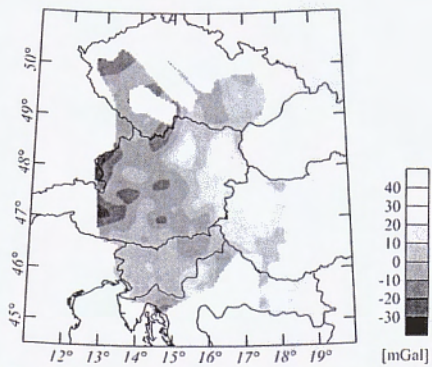

Fig. 18 Bouguer gravity residuum (dgB3) after removing the effect of the whole crust.

Figure 17 shows the depth map of the Moho calculated from the time map (Figure 5) and the interval velocities shown in Figure 16.

Finally, we calculated the gravity effect of the lower crust between Z = 10 km and the Moho on the basis of the improved P-wave velocities and their transformation to densities. The final gravity residuum (dgB3) after removing the effect of the whole crust is shown in Figure 18. The standard deviation of dgB3 is 11 mGal, the standard deviation of the Bouguer anomaly without any corrections for the crust (dgB0) has been 30 mGal. The residuum dgB3 does not show any more the signature of the topography or the Moho structure.

8 Isostasy

A density model of the lithosphere should also represent a reasonable solution for isostasy. A map of the isostatic anomaly of the Eastern Alps was calculated by Wagini et al. (1988). The residuals vary between -25 mGal and +25 mGal with an average value of +8 mGal. Meurers (1996) points out that density variations in the upper crust may significantly change the isostatic residual and he concludes that the Eastern Alps are at least near an isostatic equilibrium. Braitenberg et al. (2002) and Ebbing (2004) come to the conclusion that the internal crustal loads contribute to the isostatic equilibrium in the same order of magnitude as the topographic loads in the area of TRANSALP. Again the Airy-isostatic residual shows a strong correlation with tectonics and the near surface density distribution. Furthermore, calculations of the flexural rigidity result in relatively low values.

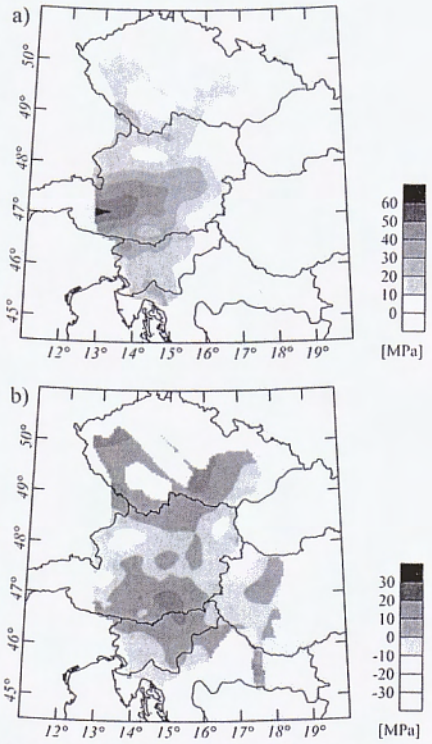

Fig. 19 Vertical loading stress, derived from the loads given by our density model at **(a)** Z = 0 km and **(b)** Z = 50 km. The values at Z = 50 km are relative to the reference lithosphere.

The study of Lillie et al. (1994) in the Eastern Alpine - Western Carpathian - Pannonian Basin region demonstrate that the lithosphere - asthenosphere boundary must be included into the gravimetric modeling to achieve isostatic equilibrium.

From these findings we conclude, the vertical loading stress at Z=50 km (a level below the orogen roots), derived from the loads given by our density model should be near an Airy-isostatic equilibrium. Long wave length deviations from equilibrium should find their compensation in the lower lithosphere and asthenosphere (Lillie et al. 1994).

Figure 19 shows the vertical loading stresses at Z=0 km (a) and Z=50 km (b). The load of the masses above Z=0 km were calculated from a smoothed topography and a constant density of 2670 kg m^{-3}. The values of the vertical loading stresses at Z=50 km are calculated from the loads given by our 3D density model relative to the reference lithosphere defined in paragraphs 4 and 5. The standard deviation from isostatic equilibrium at Z=50 km is +/- 6 MPa. Ebbing et al. (2005) derived deviations from isostatic equilibrium in the same order of magnitude in the central part of the Eastern Alps (TRANSALP) at depth levels 60 - 300 km from a high resolution 3D density model.

9 Conclusions and Future Plans

The presented work is based on a preliminary 3D seismic model and Bouguer gravity map of the Eastern Alpine crust. It has therefore the character of pilot study. The P-wave velocity of the crust was mainly determined by diving wave tomography. In a considerable part of the investigation area the penetration depth of this method was not deep enough to achieve sufficient information on the velocity of the lower crust.

The implementation of gravity data resulted in a well-constrained solution for the P-wave velocity of the lower crust in the interval between Z=10 km and the Moho. The variations of the seismic velocities of the crust, the Moho topography and the Bouguer gravity residual after stripping the uppermost 10 km of the crust and removing the influence of the Moho topography (dgB2) can be related to tectonic provinces and geodynamic processes to some extent.

Conversion of the seismic model constrained by gravity to a density model using the relations from Christensen and Mooney (1995) and subtraction of the gravity effect of this model from the observed Bouguer gravity (dgB0) results in a residuum (dgB3) that reduces the variance of dgB0 by 86% (Figure 18). The vertical loading stress at the depth level Z=50 km corresponding to this density model (Figure 19b) shows only little variations. Adjustments of the average densities of the 50 km lithospheric columns by less than 1% could restore Airy-isostatic equilibrium.

Despite the good fit of our velocity and density model the final residuals of gravity and the deviation from isostatic equilibrium show patterns, which again could be related to tectonic structures and processes. However, before we consider these relations we plan to improve our results by the use of an upgraded gravity map, which will be available for our investigation area in the near future (Meurers, personal communication). Furthermore, we will implement the surface density map (Steinhauser et al. 1984). The evaluation of S-wave velocities will provide better constraints on the mineralogy. Consideration of thermal flux and temperature as well as other velocity density relations (f.e. Sobolev and Babeyko 1994) will be necessary too. Also teleseismic models of the lower lithosphere and asthenosphere (f.e. Lippitsch et al. 2003) should be incorporated to model the deep structures.

Acknowledgements

This work is part of the ALP 2002 and ALPASS projects and has been funded by the Austrian Academy of Sciences and the Austrian Science Fund, project P15576-N06. We say our sincere thanks to C. Braitenberg and M.G. Doufexopoulou for their thorough reviews that helped to improve the paper and to A.J. Gil and F. Sansó for their efforts as editors.

Members of the CELEBRATION 2000 and ALP 2002 Working Groups

S. Acevedo, K. Aric, M. Behm, A. Belinsky, F. Bleibinhaus, T. Bodoky, E. Brückl, R. Clowes, W. Chwatal, W. Czuba, E. Gaczyński, H. Gebrande, A. Gosar, M. Grad, H. Grassl, A. Guterch, Z. Hajnal, S. Harder, E. Hegedüs, S. Hock, V. Hoeck, P.Hrubcová, T. Janik, G. Jentzsch, P. Joergensen, A. Kabas, G. Kaip, K. Komminhaho, G.R. Keller, F. Kohlbeck, S. Kostiuchenko, D. Kracke, K.C. Miller, A. Morozov, J. Oresko, K. Posgay, E.-M. Rumpfhuber, C. Schmid, R. Schmöller, O. Selvi, C. Snelson, A. Špicák, P. Środa, F. Sumanovac, E. Takács, H. Thybo, T. Tiira, C. Tomek, C. Ullrich, J. Vozár, F. Weber, M. Wilde-Piórko, J. Yliniemi.

References

Aric, K., et al. (1987). Seismological studies in the Eastern Alps. In: H.W. Flügel, P. Faupl (Ed.): Geodynamics of the Eastern Alps. Franz Deuticke Verlag.

Behm, M. (2006). Accuracy and resolution of a 3D seismic model of the Eastern Alps. Ph.D.-Theses. Vienna University of Technology, Vienna.

Behm, M., E. Brückl, W. Chwatal, H. Thybo and CELEBRATION 2000 Working Group, ALP 2002 Working Group (2004). Seismic structure of the Eastern Alps - evidence for a "Pannonian" microplate. Poster Presentation at IGC Florence, Italy, August 20-28, 2004.

Bleibinhaus, F., E. Brückl, A. Gosar, M. Grad, E. Hegedüs, P. Hrubcová, G.R. Keller, F. Sumanovac, J. Yliniemi and ALP 2002 Working Group (2004). Alp 2002 Experiment - 2D Raytracing modelling and seismic tomography of selected profiles. Poster Presentation at IGC Florence, Italy, August 20-28, 2004.

Braitenberg C., J. Ebbing, H.-J. Götze (2002). Inverse modelling of elastic thickness by convolution method - the Eastern Alps as a case example. Earth and Planetary Science Letters, 2002, 387-404.

Braitenberg C., F. Pettenati, M. Zadro (1997). Spectal and classical methods in the evaluation of Moho undulations from gravity data: the NE-Italian Alps and isostasy. Journal of Geodynamics, 23, 5-22.

Brückl, E., T. Bodoky, A. Gosar, M. Grad, A. Guterch, Z. Hajnal, E. Hegedüs, P. Hrubcová, G.R. Keller, A. Špičák, F. Sumanovac, H. Thybo, F. Weber and ALP 2002 Working Group (2003a). ALP 2002 seismic experiments. Stud. Geoph. Geod., 47 (2003), 671-679.

Brückl E., M. Behm, W. Chwatal (2003b). The application of signal detection and stacking techniques to refraction seismic data. Oral Presentation at AGU, San Francisco, 08-12 December 2003.

Čermak, V., Balling, N., Della Vedova, B., Lucazeau, F., Pasquale, V., Pellis, G., Schulz, R., and Verdoya, M. (1992). Heat-flow density. In D. Blundell, R. Freeman, and S. Mueller, editors, A Continent Revealed: The European Geotraverse. Cambridge University Press.

Červený, V. and I. Psencik, (1984). Documentation of Earthquake Algorithms. SEIS83 - Numerical modeling of seismic wave fields in 2-D laterally varying layered structures by the ray method. E. R. Engdahl edit., Report SE-35, Boulder, 36-40.

Christensen, N.I. and W.D. Mooney (1995). Seismic velocity structure and composition of the continental crust: A global view, J. Geophys. Res., 100, 97619788.

Christensen, N. (1996). Poisson ratio and crustal seismology, J. Geophys. Res 101, 3139-3156.

Dal Moro G., C. Braitenberg, and M .Zadro (1998). Geometry and mechanical and crustal properties in NE Italy based on seismic and gravity data. B olletino di Geofisica Teorica ed Applicata,Vol. 39, N.1, 37-46.

Ebbing, J. (2002). 3-D Dichteverteilung und isostatisches Verhalten der Lithosphäre in den Ostalpen. Thesis, Freie Universität Berlin, 143.

Ebbing, J. (2004). The crustal structure of the Eastern Alps from a combination of 3D gravity modelling and isostatic investigations. Tectonophysics, 380/1-2, 80-104.

Ebbing J., C. Braitenberg, H.-J. Götze (2001). Forward and inverse modell ing of gravity revealing insight into crustal structures of the Eastern Alps. Tectonophysics, 337/3-4, 191-208.

Ebbing J., C. Braitenberg, H.-J. Götze (2005). The lithospheric density structure of the Eastern Alps. Tectonophysics, in press (Transalp special volume).

Giese, P., et al. (1976). Explosion Seismology in Central Europe. Eds. P. Giese, C. Prodehl, A. Stein. Springer Verlag Berlin, Heidelberg, New York.

Graßl, H. (1999). NESTMK - Ein Tiefenseismikprofil in der Nordoststeiermark. Dissertation, Institut für Geophysik, Montanuniversität Leoben, Mai 1999.

Graßl, H., F. Neubauer, K. Millhan, F. Weber, (2004). Seismic image of the deep crust at the eastern margin of the Alps (Austria): indications for crustal extension in a convergent origin. Tectonophysics 380, 105-122.

Guterch, A., M. Grad, G.R. Keller, K. Posgay, J. Vozár, A. Špičák, E. Brueckl, Z. Hajnal, H. Thybo, O. Selvi, and CELEBRATION 2000 Experiment Team (2003). CELEBRATION 2000 Seismic Experiment, *Stud. Geoph. Geod.*, 47, 659-669.

Hrubcová P, P. Sroda, A. Špičák and CELEBRATION 2000 Working Group (2005). Crustal and uppermost mantle structure of the Bohemian Massif based on CELEBRATION 2000 data. J. Geophys. Res, in press.

Kraiger, G. and N. Kühtreiber (1992). Preliminary results of a new Bouguer Map of Austria. Geodesy and Physics of the Earth: Geodetic Contributions to Geodynamics, 7 th Symposium Nr. 112, 5-10 October, Potsdam. Eds. H. Montag and C. Reigber: Springer-Verlag, p.133

Lillie, R.J., M. Bielik, V. Babuska, and J. Plomerova (1994). Gravity modelling of the lithosphere in the Eastern Alpine - Western Carpathian - Pannonian Basin region. Tectonophysics, 231, 215-235.

Lippitsch, R. (2002). Lithosphere and Upper Mantle P-Wave Velocity Structure Beneath the Alps by High-Resolution Teleseismic Tomography. Ph.D.-Thesis, Swiss Federate Institute of Technology, Zürich.

Lippitsch, R., E. Kissling, J. Ansorge, (2003). Upper mantle structure beneath the Alpine orogen from high-resolution teleseismic tomography, Journal of Geophysical Research, 108, B8, 2376, doi: 10.1029/2002JB002016

Meurers, B. (1996). Investigation of the isostatic anomaly of the Eastern Alps. Acta Geod. Geophys. Hung., 31 (3-4), 389-403

Meurers, B. (1993). Die Böhmische Masse Österreichs im Schwerefeld. 6. Int. Alpengrav. Koll., Leoben 1993, Österr. Beitr. Met. Geoph., 8, 69-81.

Meurers, B., D. Ruess, P. Steinhauser, (1987). The Gravimetric Alpine Traverse. In: Flügel, H., and Faupl, P. (Editors): Geodynamics of the Eastern Alps. Deuticke, Vienna, 334-344.

Nagy, D. (1996). The gravitational attraction of right angular prism. Geophysics 31, pp. 362371, 1966

Posgay, K., et al. (1996). International deep reflection survey along the Hungarian Geotraverse, Geoph. Trans. 40 (1-2), 1-44.

Ratschbacher, L., Frisch, W., Linzer, H.-G., and Merle, O. (1991). Lateral extrusion in the Eastern Alps, Part II: Structural analysis. Tectonics, 10, 256-272.

Sachsenhofer, R. (2001). Syn- and post-collisional heat flow in the Cenozoic Eastern Alps. Int. J. Earth Sciences (Geol. Rundsch.), 90, 579-592.

Scarascia, S. and R. Cassinis, (1997). Crustal structures in the central-eastern Alpine sector: a revision of the available DSS data. Tectonophysics 271, 157-188.

Schmid, S., Fügenschuh, B., Kissling, E., and Schuster, R. (2004). Tectonic map and overall achitecture of the Alpine orogen. Eclogae Geologicae Helvetiae, Swiss Journal of Geosciences, 97/1, 93-117.

Senftl, E. (1965). Scherekarte von Österreich, Bouguer-Isanomalen, 1:1 Mill., Bundesamt für Eich- u. Vermessungswesen, Wien.

Sobolev, S.V and A.Y. Babeyko, (1994). Modelling of mineralogical composition, density and elastic wave velocities in anhydrous magamatic rocks. Surveys in Geophysics 15, 515-544.

Steinhauser, P., D. Ruess, D. Zych, H. Haitzmann, G. Walach (1984). The geoid in Austria: Digital models of mean topographic heights and rock densities. Proc. 18th Gen. Ass. IUGG, IAG, Vol. I, 322-338.

Tomek, C. (1993a). Deep crustal structure beneath the central and inner West Carpathians. Tectonophysics 226, p. 417-431.

Tomek, C. (1993b). Subducted continental margin imaged in the Carpathians of Czechoslovakia. Geology, v.21, p. 535-538.

Transalp Working Group (2002). First deep seismic reflection images of the Eastern Alps reveal giant crustal wedges and transcrustal ramps. Geophys. Res. Let. 29 (10), 10.1029/2002GL014911, 92-1 - 92-4.

Wagini, A., Steinhauser, P., Meurers, B. (1988). Isostatic residual gravity map of Austria. USGSA, Open file report 87-402.

Weber, F., R. Schmöller, R.K. Frühwirth (1996). Results of a deep reflection seismic measurement south of Rechnitz/Burgenland/Austria. Geophys. Trans., 40, 79-93.

Yan, Q.Z., J. Mechie, (1989). A fine section through the crust and lower lithosphere along the axial region of the Alps. Geophysical Journal 98, 465-488.